

Magic Polyicosahedral Core-Shell Clusters

G. Rossi,¹ A. Rapallo,² C. Mottet,³ A. Fortunelli,⁴ F. Baletto,⁵ and R. Ferrando¹

¹*INFN and IMEM/CNR, Dipartimento di Fisica, Via Dodecaneso 33, Genova, I16146, Italy*

²*ISMAR/CNR, Via Bassini 15, Milano, I20133, Italy*

³*CRMCN/CNRS, Campus de Luminy, Marseille, F13288, France*

⁴*IPCF/CNR, Via Alfieri 1, Ghezzano, I56010, Italy*

⁵*ICTP, Strada Costiera 11, Trieste, I34014, Italy*

(Received 15 April 2004; published 2 September 2004)

A new family of magic cluster structures is found by genetic global optimization, whose results are confirmed by density functional calculations. These clusters are Ag-Ni and Ag-Cu nanoparticles with an inner Ni or Cu core and an Ag external shell, as experimentally observed for Ag-Ni, and present a polyicosahedral character. The interplay of the core-shell chemical ordering with the polyicosahedral structural arrangement gives high-symmetry clusters of remarkable structural, thermodynamic, and electronic stability, which can have high melting points (they melt higher than pure clusters of the same size), large energy gaps, and (in the case of Ag-Ni) nonzero magnetic moments.

DOI: 10.1103/PhysRevLett.93.105503

PACS numbers: 61.46.+w, 71.15.Mb

Bimetallic nanoclusters have received considerable attention recently [1] for their peculiar properties, which can be very different from those of pure clusters of their constituents [2,3], and for a variety of applications, ranging from catalysis to optics [4,5]. What renders bimetallic nanoclusters very attractive is that their properties can vary dramatically not only with size, as happens in pure nanoclusters, but also with chemical composition. Controlling their structure and chemical ordering can be the starting point to prepare the building blocks for specifically tailored cluster-assembled materials [6]. For this application, a key step is to single out magic cluster structures, namely, those structures presenting special structural, as well as electronic and thermodynamic, stability. In recent experiments [7], it has been shown that silver-nickel nanoclusters adopt a core-shell configuration, where a well-defined outer silver shell embeds a nickel core. The analysis of low-energy ion scattering data has shown that the silver shell is often of monatomic thickness, but a more precise determination of their structure is not available yet.

Here we show theoretically that there is a whole family of new magic Ag-Ni and Ag-Cu nanoclusters, which are characterized by the common structural properties of being perfect core-shell clusters and polyicosahedra (pIh). Perfect core-shell clusters have all Ag atoms on the surface and all Ni or Cu atoms inside, so that the Ag shell is of monatomic thickness. pIh are clusters built by packing elementary Ih of 13 atoms (Ih₁₃), as shown in Fig. 1. Previously [8,9], it has been shown that core-shell and multishell clusters can be kinetically favorable (but often metastable) structures in the growth of bimetallic clusters. Here we demonstrate that there is a new family of core-shell clusters of remarkable stability also from the energetic and thermodynamic point of view. In the following, a pIh of size N , made of N_1 Ag atoms and $N_2 =$

$N - N_1$ Cu or Ni atoms, and comprising m interpenetrating Ih₁₃, are referred to as (N_1, N_2) pIh ^{m} . We demonstrate that the interplay between the pIh structural ordering and the core-shell chemical ordering gives a net driving force for building up clusters of remarkable structural stability. Among these core-shell pIh we single out a few high-symmetry clusters presenting special thermodynamic and electronic stability, with high melting points and large highest occupied molecular orbital–lowest unoccupied molecular orbital (HOMO-LUMO) gaps. Some of these structures are also magnetic in their ground state.

Our computational procedure consists of several steps: (i) We model the clusters by realistic many-body atom-atom potentials [10], and search for the global energy minimum by genetic algorithm optimization [11] for some selected sizes and variable composition. (ii) At a given size, we look for the compositions corresponding to the most stable structures. (iii) We locally optimize the most significant structures using density functional theory (DFT) calculations [12] to confirm the trends obtained in (ii) and single out the clusters with high electronic stability. (iv) We check the thermodynamic stability of the magic structures by making molecular-dynamics melting simulations and calculating the temperature-dependent probabilities of the global minima by harmonic thermodynamics [13].

Why can core-shell pIh be magic structures? A driving force for the formation of high-stability clusters is the maximization of the number of nearest-neighbor bonds among the atoms. This favors compact quasispherical structures, such as the Ih₁₃ and other Ih. However, interatomic distances in Ih are different from their ideal value in the bulk crystal, and this produces an internal strain. The competition between the maximization of the bond number and the accumulation of strain determines the most favorable structures in pure systems with pair inter-

actions [14], such as Lennard-Jones (LJ) and Morse. LJ clusters of 13 atoms prefer the Ih shape, and, adding further atoms, a series of compact polyicosahedral clusters is produced at $N = 19, 23, 26, 29$ [15]. Above $N = 29$, the gain in the bond number does not compensate any more the internal strain so that LJ pIh become less favorable. For noble and transition metal pure clusters the situation is more complicated. The many-body part of the metallic bonding tends to disfavor Ih structures because it induces a significant *bond order–bond length correlation* [16], which means that the optimal bond length *increases with the coordination* of the atoms. This is exactly the

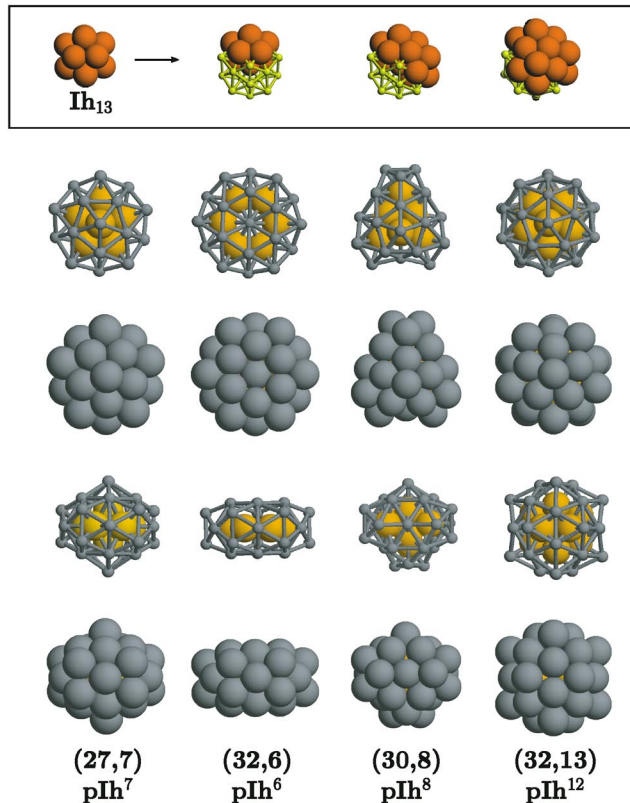


FIG. 1 (color). Magic core-shell pIh clusters. pIh clusters are built by packing elementary Ih₁₃ clusters (see also Fig. S1), as shown in the top row, where three different fragments of the pIh⁷ structure are given. From left to right, the fragments comprise one, two, and four interpenetrating Ih₁₃. Below, a selection of magic core-shell pIh is given. Each pIh is shown in four views; in two of them the Ag atoms (gray color) are represented by small points to show the arrangement of the core (Ni or Cu, orange color) atoms. The (27, 7)pIh⁷ has a decahedral Ni or Cu core of 7 atoms, and the 27 Ag atoms are placed in an anti-Mackay overlayer. The (32, 6)pIh⁶ is a *pancake* structure, with the six inner atoms placed on a regular hexagonal ring. The (30, 8)pIh⁸ is the perfect core-shell structure including the maximum number of core atoms at size 38. The (32, 13)pIh¹² is the complete anti-Mackay icosahedron of size 45, including a perfect Ih₁₃ core. It is made of 12 interpenetrating Ih₁₃ sharing the central atom as a common vertex.

opposite of what happens in Ih, where internal bonds are on the average shorter than surface bonds. In the Ih₁₃, internal bonds are 5% shorter than surface bonds. Compact pIh suffer from the same problem, since they have even more compressed internal distances, and a huge internal strain. Thus they are not expected to be of special stability for pure transition metal clusters.

However, the situation can change drastically in binary systems. In fact, substituting the internal atoms in a pure pIh cluster with *smaller atoms*, the optimal bond lengths of both internal and surface atoms may be recovered, and the strain strongly decreased. This leads naturally to the idea of *core-shell pIh clusters*, which both maximize the bond number and minimize the strain. Other important factors favoring such clusters are that the large atoms must have a strong tendency toward segregating at the surface, and possibly the two elements should have a weak tendency toward mixing or alloying in the bulk phase. All these features are present in Ag-Ni and Ag-Cu. Ni and Cu atoms are 16% and 13% smaller than Ag atoms, Ag has a strong tendency to surface segregation with respect to both Ni and Cu [17], and Ag-Ni and Ag-Cu bulk systems present very extended miscibility gaps [18]. Our results demonstrate that the Ag-Ni and the Ag-Cu systems are really suitable for building up magic core-shell pIh. We shall show that, given the size, the most stable structures are obtained at the compositions corresponding to perfect core-shell pIh.

To compare the relative stability of clusters of different sizes and compositions, we monitor the quantities Δ and Δ_2 [19] adapted to binary clusters. Δ is the excess energy with respect to N bulk atoms, divided by $N^{2/3}$:

$$\Delta = \frac{E_{\text{GM}}^{N,N_1} - N_1 \varepsilon_1^{\text{coh}} - N_2 \varepsilon_2^{\text{coh}}}{N^{2/3}}, \quad (1)$$

where N_1 and $\varepsilon_1^{\text{coh}}$ are the number and the bulk cohesive energy of Ag atoms, whereas $N_2 = N - N_1$ and $\varepsilon_2^{\text{coh}}$ are the same quantities of either Ni or Cu, and E_{GM}^{N,N_1} is the global-minimum energy at the given size and composition. Stable structures are identified by low Δ values. Δ_2 is the second difference in the energy:

$$\Delta_2^{N,N_1} = E_{\text{GM}}^{N,N_1+1} + E_{\text{GM}}^{N,N_1-1} - 2E_{\text{GM}}^{N,N_1}. \quad (2)$$

Maxima of Δ_2 indicate structures of special relative stability compared to those of the same size and nearby compositions.

We start our analysis at $N = 38$, and look for the global energy minima at varying compositions. Size 38 is magic for the regular truncated octahedron, a high-symmetry piece of fcc bulk lattice, and thus is expected to correspond to pure clusters of good stability. Plotting Δ and Δ_2 vs N_1 , for both Ag-Ni and Ag-Cu, the same conclusion follows (see Fig. 2): the minimum Δ and a high peak in Δ_2 correspond to the perfect core-shell structure which includes the maximum number of small atoms inside,

namely, 30 external Ag atoms and 8 inner Ni or Cu atoms. This structure (see Fig. 1) is a (30, 8)pIh⁸, made up of 8 interpenetrating Ih₁₃. Other perfect core-shell pIh are the (31, 7)pIh⁷ and the (32, 6)pIh⁶. The latter is a highly symmetric (group D_{6h}) *pancake* structure.

At $N = 34$, the predominance of the core-shell pIh structure is even clearer. This is the right size for forming a high-symmetry (group D_{5h}) pIh made of 7 Ih₁₃. This structure underlies most of the minima at varying compositions, and attains its maximum stability when the perfect core-shell arrangement is formed, in (27, 7)pIh⁷. It contains a compact decahedral nucleus of Ni or Cu, and all Ag atoms are placed in an anti-Mackay [20] shell (see Fig. 1). The special energetic stability of perfect core-shell pIh at $N = 34$ and $N = 38$ is nicely confirmed by our DFT calculations, whose results are reported in Fig. 2 and Table I. The atom-atom potential geometries are only slightly modified by the DFT relaxation, thus validating the accuracy of the semiempirical approach for these elements.

High-stability core-shell pIh constitute a rich family of different sized clusters. At $N = 45$ we find the so-called anti-Mackay (see [20]) Ih, (32, 13)pIh¹² which is the highest symmetry pIh. It is obtained by covering a Ni or Cu Ih₁₃ with a complete anti-Mackay Ag shell. Moreover, there is a series of perfect core-shell pIh

made of fragments of this anti-Mackay pIh¹². They are shown in the auxiliary material [21]. All the perfect core-shell pIh are well separated in energy from their homotops (homotops are defined as clusters of the same size, structure, and composition, and differ only in the chemical ordering). This separation is due to the high energetic cost of placing an Ag atom in the cluster core.

Among this family of core-shell pIh, now we focus on the (27, 7)pIh⁷, which from Fig. 2 and Table I seems to have the most intriguing properties. For Ag-Cu, this cluster has a large gap (0.82 eV), indicating a strong electronic stability, and no magnetic moment. For Ag-Ni, the gap is still rather large (0.81 and 0.46 eV in the majority and the minority spin, respectively), and the ground state has a non-negligible magnetic moment. In both cases, the (27, 7)pIh⁷ is also of remarkable thermodynamic stability, as follows from the analysis of its melting behavior. In fact (see Fig. 3), this core-shell cluster melts at considerably *higher* temperature than pure Ag, Cu, and Ni clusters in the same size range. This is at variance with the behavior of Ag-Cu and Ag-Ni bulk systems, where the melting point is depressed at mixed compositions [18]. The thermodynamic stability of the (27, 7)pIh⁷ follows from two factors. First, this cluster is well separated from higher isomers [22], by at least 0.3 eV for Ag-Cu and 0.45 eV for Ag-Ni according to the atom-atom potential, but the DFT calculations give a much larger separation, of more than 0.8 eV. Second, our harmonic thermodynamics calculations show that

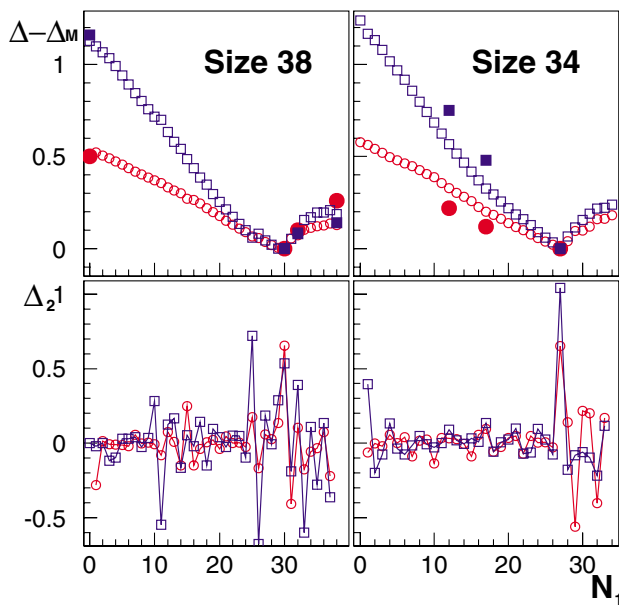


FIG. 2 (color online). Δ and Δ_2 (in eV) for clusters of fixed size vs the number of Ag atoms N_1 . Δ_M is the minimum value of Δ at the given size. Circles and squares refer to Ag-Cu and Ag-Ni, respectively. Open symbols refer to the atom-atom potential results, while full symbols refer to the DFT results. Minima in Δ and maxima in Δ_2 both concur to single out the most stable structures, which are the perfect core-shell (30, 8)pIh⁸ and (27, 7)pIh⁷ (see Fig. 1) at sizes 38 and 34, respectively.

TABLE I. DFT calculations results. Values of spin (S) and HOMO-LUMO gap (in eV) for alpha/beta electrons. The symbol “JT” signals a Jahn-Teller system, with a degenerate HOMO. Pictures of the (17, 17)pIh⁷ and (12, 22)pIh⁷ are shown in [21]. For pure clusters, the DFT relaxation shows that defected decahedral structures are slightly lower in energy than the truncated octahedra.

System	Size	Cluster	S	Gap
Ag	38	Truncated octahedron	1	0.39/0.35 JT
Cu	38	Truncated octahedron	1	0.61/0.56 JT
Ni	38	Truncated octahedron	16	0.21/0.03 JT
Ag-Cu	38	(32, 6)pIh ⁶	0	0.34/0.34
	38	(30, 8)pIh ⁸	0	0.26/0.26
	34	(27, 7)pIh ⁷	0	0.82/0.82
	34	(17, 17)pIh ⁷	0	0.94/0.94
	34	(12, 22)pIh ⁷	0	0.88/0.88
	45	(32, 13)pIh ¹²	2.5	0.49/1.00
Ag-Ni	38	(32, 6)pIh ⁶	0	0.09/0.09
	38	(30, 8)pIh ⁸	0	0.05/0.05
	34	(27, 7)pIh ⁷	3.5	0.81/0.46
	34	(17, 17)pIh ⁷	6.5	0.19/0.07
	34	(12, 22)pIh ⁷	7	0.26/0.07 JT
	45	(32, 13)pIh ¹²	16	0.21/0.03 JT

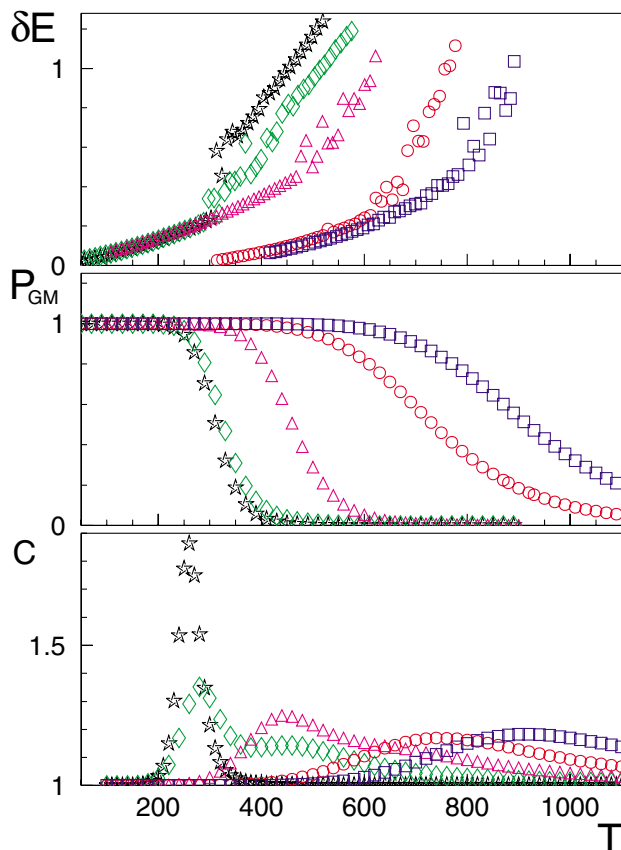


FIG. 3 (color online). Melting of pure clusters and of core-shell pIh. The top panel shows the molecular-dynamics caloric curves δE (in eV) vs temperature T (in K), where $\delta E = E - E_{GM} - 3(N-1)k_B T$, namely, δE is the total cluster energy minus the global-minimum energy E_{GM} and the harmonic contribution $3(N-1)k_B T$. The middle panel reports p_{GM} which is the probability of finding the cluster in its global-minimum structure as a function of T . The bottom panel reports the vibrational specific heat c per degree of freedom (in units of the Boltzmann constant k_B). p_{GM} and c are calculated in the harmonic superposition approximation. Stars, diamonds, and triangles refer to pure Ag_{38} , Cu_{38} , and Ni_{38} clusters; circles and squares refer to the $(27, 7)pIh^7$ of Ag-Cu and Ag-Ni. Core-shell pIh melt considerably higher than pure clusters.

the entropic contributions to the free energy are favorable to the $(27, 7)pIh^7$ structure.

The electronic and magnetic properties of this new family of magic clusters can be of great interest, and are currently under investigation. For example, the large gap and the stability of the Ag-Cu $(27, 7)pIh^7$ make this cluster potentially suitable for applications in optoelectronic and single-electron tunneling devices. On the other hand, the same cluster is a promising candidate for single-molecule magnetism in the case of Ag-Ni. Finally, since the requirements for these structures are of quite general character (size mismatch, large atoms segregating at the surface with respect to small atoms, possibly a weak

tendency to mix in the bulk phase), we expect that magic core-shell polyicosahedra are likely to be encountered in a large variety of binary metallic systems, for example, Ag-Co, Au-Ni, Au-Co, and (with a weaker tendency) Ag-Pd and Au-Cu.

The authors thank J. P. K. Doye and R. L. Johnston for a critical reading of the manuscript. A. F. and R. F. acknowledge financial support from the CNR for the project SSA-TMN in the framework of the ESF EUROCORES SONS. A. F. acknowledges the INSTM for a grant at CINECA.

- [1] J. Jellinek and E. B. Krissinel, in *Theory of Atomic and Molecular Clusters*, edited by J. Jellinek (Springer, Berlin, 1999), pp. 277–308.
- [2] T. Shibata *et al.*, *J. Am. Chem. Soc.* **124**, 11 989 (2002).
- [3] S. Darby *et al.*, *J. Chem. Phys.* **116**, 1536 (2002).
- [4] A. M. Molenbroek, S. Haukka, and B. S. Clausen, *J. Phys. Chem. B* **102**, 10 680 (1998).
- [5] U. Kreibitz and M. Vollmer, *Optical Properties of Metal Clusters* (Springer, Berlin, 1995).
- [6] P. Jensen, *Rev. Mod. Phys.* **71**, 1695 (1999).
- [7] M. Gaudry *et al.*, *Phys. Rev. B* **67**, 155409 (2003).
- [8] F. Baletto, C. Mottet, and R. Ferrando, *Phys. Rev. B* **66**, 155420 (2002).
- [9] F. Baletto, C. Mottet, and R. Ferrando, *Phys. Rev. Lett.* **90**, 135504 (2003).
- [10] Form and parameters are given in [8,9].
- [11] For a general description of genetic algorithms for binary clusters optimization see [3].
- [12] DFT calculations are carried out by the DFT module of the NWCHEM package [R. A. Kendall *et al.*, *Comput. Phys. Commun.* **128**, 260 (2000)]. $(7s6p6d)/(5s3p2d)$ Gaussian-type orbital basis sets and effective core potentials are used for all elements. A charge density fitting basis is used for the Coulomb integrals (courtesy of Dr. F. Weigend). More details are in E. Aprà and A. Fortunelli, *J. Chem. Phys.* **107**, 2394 (2003).
- [13] J. P. K. Doye and F. Calvo, *Phys. Rev. Lett.* **86**, 3570 (2001).
- [14] J. P. K. Doye, D. J. Wales, and R. S. Berry, *J. Chem. Phys.* **103**, 4234 (1995).
- [15] See the Cambridge Cluster Database, <http://www-wales.ch.cam.ac.uk/CCD.html>.
- [16] L. Pauling, *The Nature of the Chemical Bond* (Cornell University Press, New York, 1960).
- [17] J.-M. Roussel *et al.*, *Phys. Rev. B* **55**, 10 931 (1997).
- [18] M. Hansen, *Constitution of Binary Alloys* (McGraw-Hill, New York, 1958).
- [19] C. L. Cleveland and U. Landman, *J. Chem. Phys.* **94**, 7376 (1991).
- [20] J. A. Northby, *J. Chem. Phys.* **87**, 6166 (1987).
- [21] See EPAPS Document No. E-PRLTAO-93-057434 for pictures of core-shell polyicosahedra structures. A direct link to this document may be found in the online article's HTML reference section. The document may also be reached via the EPAPS homepage <http://www.aip.org/pubservs/epaps.html> or from <ftp.aip.org> in the directory /epaps/. See the EPAPS homepage for more information.
- [22] D. D. Frantz, *J. Chem. Phys.* **115**, 6136 (2001).